

# Mössbauer and metallographic analysis of borided surface layers on Armco iron

M. CARBUCICCHIO, L. BARDANI  
*Institute of Physics, University of Parma, Italy*

G. PALOMBARINI  
*Institute of Metallurgy, University of Bologna, Italy*

Armco iron samples boronized at 850 and 1000° C in crystalline boron powder have been studied. Scattering and transmission Mössbauer measurements, supported by optical and electron scanning metallography and by X-ray diffraction analysis, enabled the surface phases to be identified, the multi-layer structure of the coatings to be defined and the average thickness of each layer to be measured. In addition to an inner Fe<sub>2</sub>B layer and to an intermediate FeB layer, the presence of an outer layer of a third phase richer in boron than FeB has been ascertained in the boride coatings. The morphology of the reaction products and their mechanical consistency have also been examined and discussed.

## 1. Introduction

Boriding is a thermochemical diffusion process which is more effective than carburizing or nitriding in order to obtain increased surface hardness and reduced friction properties, especially when treating steels, provided that borides are formed at the surface of the treated materials. The most important feature of the process is the improvement one may obtain both in adhesive wear [1, 2] and in abrasive wear [3, 4], in a number of practical circumstances where metal surfaces are rubbing against an antagonist solid material. Furthermore, the possibility exists of substituting expensive, special alloys with common, borided steels if a high mechanical strength is not required in the substrate. The main restrictions on the applicability of the treatment are associated with the inherent brittleness of the borided layers.

A predominant number of studies have been published on the general techniques of steel boriding and on the properties and uses of the surface layers so produced. More refined materials such as Armco iron or high purity iron have been often utilized as reference materials, to which compare carbon and alloy steels with the major aim of establishing what materials are better suitable for boriding. Relevant papers concerning Armco iron or high purity iron are summarized in the following.

The character and the preferential paths of the boron dissolution in  $\alpha$ -iron were studied by Chomka *et al.* [5] by means of internal friction measurements on wires of Armco iron borided at 850° C in vacuum and in contact with amorphous boron powder. Krishtal and Grinberg [6] examined the changes that a boron diffusion causes in the microstructure of a coarse-grained iron containing traces of C, S, N, Mn, Ni and Ti. By microscopic and X-ray diffraction analyses, Katagiri *et al.* [7, 8] investigated both the phases occurring on iron specimens exposed to boronizing gas mixtures, and the rate of growth of the surface layers. In a series of papers dealing with Armco iron, Lyakhovich and co-workers [9-12] studied the morphology, the rate of growth, the residual stresses, the textures and the anisotropy of the thermal expansion of borided layers. It is worth noting that the same preferred orientations found by Lyakhovich *et al.* [10] in Fe<sub>2</sub>B layers, i.e. [001] crystallographic direction preferentially oriented normal to the external surface, has been observed very recently by Casadesus *et al.* [13]. The effects of temperature, time and boronizing media on the structure and the rate of Armco iron boriding have been investigated by Kastner and Przybylowicz [14].

The present work is concerned specifically with the early stages of the boriding of Armco iron. For

this purpose, the diffusion treatments were performed with crystalline boron powder to make the boronizing process slower. A growth of rather thin borided layers being expected, the Mössbauer scattering technique described elsewhere [15] appeared to be the most appropriate one for this study. The composition and the structure of the reaction products and of the underlying transition zone can be investigated, in fact, in a fully non-destructive way by detecting the electromagnetic radiation or the electrons associated with the nuclear resonant absorption. In this way, depending on the penetration range of the measured radiation, Mössbauer spectra can be obtained for surface layers of different thickness. Moreover, by selecting the energy of the conversion electrons, it is possible to analyse surface layers thinner than their penetration range. In particular for iron, surface layers  $\sim 30\ \mu\text{m}$ ,  $\sim 20\ \mu\text{m}$  or  $\sim 300\ \text{nm}$  thick can be analysed by detecting the 14.4 keV  $\gamma$ -radiation the 6.4 keV X-rays or all the electrons, respectively. Moreover, by selecting the electron energy in the range from 5.4 up to 7.3 keV (conversion electrons), surface layers of thickness variable from 10 up to 180 nm can be analysed.

The spectroscopic results were supported by X-ray diffraction analyses and metallographic observations.

## 2. Experimental procedures

### 2.1. Materials and thermal treatments

Armco iron specimens of about  $20 \times 10 \times 1\ \text{mm}^3$  were drawn from hot-rolled sheets, subjected to wet abrasion on a 600 grit SiC paper, and annealed 15 h at  $1000^\circ\text{C}$  in a vacuum better than  $10^{-3}\ \text{Pa}$  to minimize decarburizing. The metal, 99.89 wt % pure, contained C 0.01 wt %, S 0.03, P 0.01, Mn 0.015, Si 0.01 and As 0.005 as main impurities. The annealed sheets were surface finished again on the abrasive paper and then boronized.

As boronizing medium, a crystalline powder containing B 95 wt % and O, N, Mg, Fe and Si as main impurities was employed. It was previously ascertained that boron diffused from the powder into the iron, provided time and temperature of contact were held high enough. This contradicts the view of Grishin and Sentyurev [16] who, while studying the vacuum boriding of an austenitic 18Cr–10Ni stainless steel at 900 to  $1000^\circ\text{C}$  in contact with boron powders, asserted that hardly any boron is transferred to steels from a crystalline powder. These authors did not succeed in revealing

boron in their stainless steel specimens after a 3 h treatment at  $1000^\circ\text{C}$  in crystalline boron powder.

In order to limit the presence of oxidizing agents in the furnace, prior to be utilized, the boron powder was carefully degassed by heating 5 h at  $1000^\circ\text{C}$  under high vacuum, cooled at room temperature and then saturated with pure argon. The Armco iron specimens were placed in a boat of recrystallized alumina, covered on all sides with the argon-saturated powder and heated in vacuum for times up to 24 h at  $850^\circ\text{C}$  and 15 h at  $1000^\circ\text{C}$ . Therefore, the boronizing was performed on both the  $\alpha$ - and the  $\gamma$ -allotropic forms of the iron.

### 2.2. Mössbauer measurements

The Mössbauer measurements were carried out both in transmission and in scattering geometry. The transducer was of electromechanical type working at constant acceleration and the spectra were recorded with a multi-channel analyser operating in time mode. The source was a 15 mCi  $^{57}\text{Co}$  diffused in a Rh matrix.

The scattering spectra were measured by utilizing the apparatus described elsewhere [15] and by detecting some of the radiations emitted as a consequence of the  $^{57}\text{Fe}$   $\gamma$ -resonant absorption, i.e.:

- (i) the 6.4 keV X-rays associated with internal conversion, whose penetration range in iron is  $\sim 20\ \mu\text{m}$ ;
- (ii) all the back-scattered electrons, whose maximum escape depth in iron is  $\sim 300\ \text{nm}$ ;
- (iii) only the conversion electrons in the energy range from 6 up to 7.3 keV. In this case the analysed depth is  $\sim 100\ \text{nm}$ .

It should be noted that, when measuring back-scattering Mössbauer spectra, one must take into account the radiation escape probability as a function of the crossed depth [17–19]. It follows that equal layers at different depths contribute in a different way to the Mössbauer spectra and that most of the contribution becomes from surface layers thinner than the maximum penetration depth of the detected radiation. As an example, in the energy range from 6 up to 7.3 keV (iii) the 50% of the detected conversion electrons arises, for iron, from an outer layer  $\sim 30\ \text{nm}$  thick [17]. On the other hand, according to the empirical formula of Cosslett and Thomas [20], the escape depths for different phases can be assumed to be proportional to the density of the phase and their

values can be estimated from the mean free path of the conversion electrons in pure iron.

The choice of the probing depths in this work was determined by the natural abundance (2%) of  $^{57}\text{Fe}$  in the samples and by the limited practical interest of borided surface layers thinner than 50 nm. The spectra were computer-fitted assuming Lorentzian line shapes and using a least squares fit programme.

### 2.3. Metallography and X-ray diffraction analysis

The surfaces of the boronized specimens were observed under a scanning electron microscope Jeol type JSM-P14, and the morphology of the reaction products was investigated. Fractographic observations were also carried out to point out the internal structure of the coatings. X-ray diffraction analyses were performed both prior and after mechanical descaling of surface layers, utilizing a Seifert X-ray generator, a goniometer of 0.4 m diameter and the  $\text{CuK}\alpha$  radiation of 0.15418 nm wavelength. Finally, cross-sections of the boronized specimens were metallographically prepared and examined under a Reichert MeF optical microscope.

## 3. Results and discussions

### 3.1. Mössbauer spectra

Fig. 1a shows the room temperature spectrum (measured by detecting the 6.4 keV X-radiation) of an Armco iron sample annealed for 15 h at 1000°C in vacuum, surface finished as described previously and assumed as a reference material. The relative parameters are listed in Table I.

The same sample, after boronizing at 850°C for times up to 24 h, does not display any appreciable change in the Mössbauer spectra relative both to the bulk (X-ray spectrum) and to a thin surface layer (electron spectrum). The last one is reported in Fig. 1b and its Mössbauer parameters are listed in Table I. This spectrum gives information on a surface layer  $\sim 300$  nm thick, which represents the maximum penetration range of the detected electrons. However, it is worth noting that the 65% of the electrons arises from within a surface layer 50 to 60 nm thick, as escape depth calibration measurements show [19]. As no change greater than the experimental error is detectable between the spectra of Fig. 1a and b, one can say that boronizing Armco iron with crystalline boron powder at 850°C up to 24 h does not affect the material deeper than  $\sim 30$  nm from the external

surface. This observation does not exclude the possibility that boron has diffused in  $\alpha$ -iron beyond a depth of 30 nm during boronizing at 850°C. The maximal solubility of boron in  $\alpha$ -iron, in fact, is only 10 to 15 ppm by weight at 850°C [21]. Thus, the Mössbauer spectrum of a probable iron–boron solid solution and the spectrum in Fig. 1b should have to coincide within experimental error.

Fig. 1c shows the room temperature spectrum obtained by detecting the 6.4 keV X-rays for an Armco iron sample borided 15 h at 1000°C. This spectrum has been interpreted as the superposition of two sextets (designed by  $\beta$  and  $\delta$  in the figure). Their relative parameters, listed in Table I, agree with those reported in literature for the compounds  $\text{Fe}_2\text{B}$  and  $\text{FeB}$ , respectively [22–27].

It is worth noting that, at the velocities corresponding to the  $3/2 \rightarrow 1/2$  and  $-3/2 \rightarrow -1/2$  transitions of Armco iron, this spectrum (Fig. 1c) shows two little shoulders (indicated with arrows). This fact suggests that, in a  $\sim 20 \mu\text{m}$  thick surface layer, the unaffected substrate of Armco iron begins to be detectable. All these observations agree with the well-known fact that  $\text{Fe}_2\text{B}$  and  $\text{FeB}$  grow on iron and its alloys as surface layers, and further indicate that in this case the boride thickness does not exceed  $20 \mu\text{m}$ .

Fig. 1d shows the room temperature spectrum of the same sample as in Fig. 1c, measured this time by detecting conversion electrons in the energy range from 6 up to 7.3 keV. This spectrum can be interpreted as the superposition of two sextets ( $\delta$  and  $\epsilon$ ), whose parameters are listed in Table I. As one can see, the parameters relative to the sextet  $\delta$ , measured by detecting both the X-rays (Fig. 1c) and the conversion electrons (Fig. 1d), coincide within experimental error. Therefore, in a  $\sim 100$  nm thick surface layer,  $\text{FeB}$  is still present while  $\text{Fe}_2\text{B}$  is absent, as the lack of the sextet  $\beta$  in Fig. 1d demonstrates. This indicates that  $\text{Fe}_2\text{B}$  is situated in the inner part of the surface layer grown on Armco iron borided with crystalline boron powder for 15 h at 1000°C, while  $\text{FeB}$  lies more externally.

The sextet  $\epsilon$  does not appear in Fig. 1c, which means that it arises from a very thin surface film giving no significant contribution to spectra relative to thicker layers. This very thin film can be attributed to a  $\text{FeB}_x$  compound with  $x > 1$ . This interpretation is supported by the following considerations:

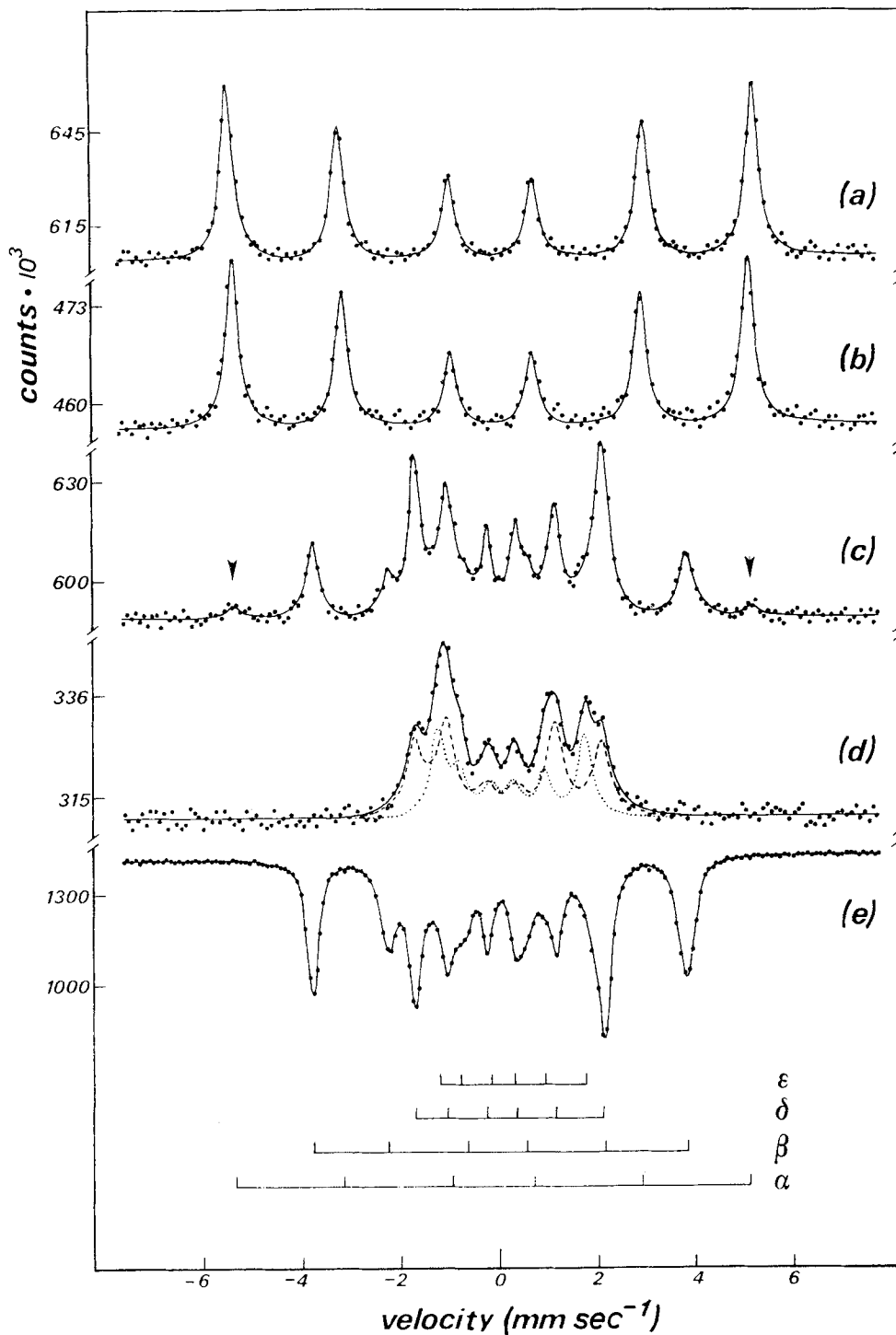


Figure 1 Room temperature Mössbauer spectra for: (a) Armco iron before boronizing (6.4 keV X-rays), (b) Armco iron boronized for 24 h at 850° C (0 to 7.3 keV electrons), (c) Armco iron borided for 15 h at 1000° C (6.4 keV X-rays), (d) Armco iron borided for 15 h at 1000° C (6 to 7.3 keV conversion electrons), (e) detached surface film from Armco iron borided for 15 h at 1000° C (14.4 keV  $\gamma$ -rays: transmission). Zero velocity is referred to Rh.

T A B L E I Mössbauer parameters for the measured samples: hyperfine magnetic fields ( $H_{\text{hf}}$ ) in kOe, quadrupolar splittings (QS) and isomer shifts referred to Rh (IS) in mm sec<sup>-1</sup>

Sample	Detected radiation	sextet $\alpha$			sextet $\beta$			sextet $\delta$			sextet $\epsilon$		
		$H_{\text{hf}}$ ( $\pm 3$ kOe)	QS ( $\pm 0.03$ mm sec <sup>-1</sup> )	IS ( $\pm 0.05$ mm sec <sup>-1</sup> )	$H_{\text{hf}}$ ( $\pm 3$ kOe)	QS ( $\pm 0.03$ mm sec <sup>-1</sup> )	IS ( $\pm 0.05$ mm sec <sup>-1</sup> )	$H_{\text{hf}}$ ( $\pm 3$ kOe)	QS ( $\pm 0.03$ mm sec <sup>-1</sup> )	IS ( $\pm 0.05$ mm sec <sup>-1</sup> )	$H_{\text{hf}}$ ( $\pm 3$ kOe)	QS ( $\pm 0.03$ mm sec <sup>-1</sup> )	IS ( $\pm 0.05$ mm sec <sup>-1</sup> )
Armco iron	6.4 keV X-rays	331	0	-0.11									
Armco iron boronized 24 h at 850° C	0-7.3 keV electrons	329	0	-0.11									
Armco iron borided 15 h at 1000° C	6.4 keV X-rays				237	0.09	-0.04	119	0.15	0.06			
Detached film from Armco iron borided 15 h at 1000° C	6-7.3 keV electrons							119	0.16	0.07	92	0.20	0.08
	14.4 keV $\gamma$ -rays				237	0.09	-0.03	120	0.15	0.06			

(1) an increase in boron content is reasonably expected on going from bulk towards external surface, which was in contact with the boronizing medium, and it agrees with the above measurements which found the Fe-richer phase ( $\text{Fe}_2\text{B}$ ) as the innermost reaction product;

(2) the hyperfine magnetic field ( $H_{\text{hf}}$ ) at the Mössbauer nuclei for the sextet  $\epsilon$  is the lowest measured one (Table I), and it is known that the  $H_{\text{hf}}$  at room temperature for iron–boron compounds decreases by increasing the boron content [22–29] (see also Table I).

Concerning the exact composition of this more external reaction product richer in boron than  $\text{FeB}$ , it is evident from the literature that  $\text{FeB}_2$  [30] and some stable or metastable phases increasingly rich in boron, such as  $\text{FeB}_{12}$  [31],  $\text{FeB}_{40}$  [32], and others are possibly existent. However, taking into account that the  $H_{\text{hf}}$  relative to  $\text{FeB}_x$  is not much lower than the one relative to  $\text{FeB}$  (see in Table I the sextets  $\epsilon$  and  $\delta$ , respectively), at present, and merely in a tentative way, the formula  $\text{FeB}_2$  may be suggested for the surface product responsible for the sextet  $\epsilon$  in Fig. 1d.

Area measurements, performed in order to determine the thickness of the “ $\text{FeB}_2$ ” layer, showed that the sextet  $\epsilon$  makes a 40% contribution to the spectrum in Fig. 1d. A value of  $\sim 30$  nm was hence estimated for the thickness of this more external boride layer.

The boride layers produced in 15 h at  $1000^\circ\text{C}$  have shown the tendency to easily descale parallel to the surface. More details of this behaviour will

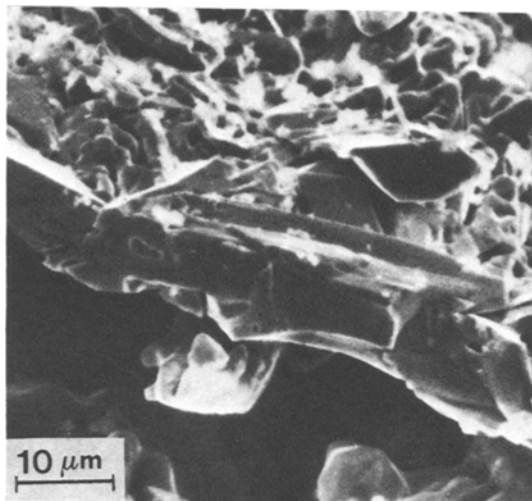


Figure 3 SEM fractograph of the outer part of a boride layer undergoing break-away on a sample treated as reported in Fig. 2.

be given in the next section. Under the scanning electron microscope (Fig. 3), a mean thickness value of  $10\ \mu\text{m}$  has been measured for the detached films. Now, Fig. 1e is of interest in that it shows the Mössbauer absorption spectrum of such a detached film. This spectrum can be interpreted as the superposition of the  $\beta$  and  $\delta$  sextets (Table I) which, in their turn, can be attributed to  $\text{Fe}_2\text{B}$  and  $\text{FeB}$ , respectively. As their contribution to the spectrum has been evaluated to be practically the same, it can be concluded that  $\text{FeB}$  has grown as a  $\sim 5\ \mu\text{m}$  thick layer at the surface of Armco iron borided for 15 h at  $1000^\circ\text{C}$ . On the other hand,

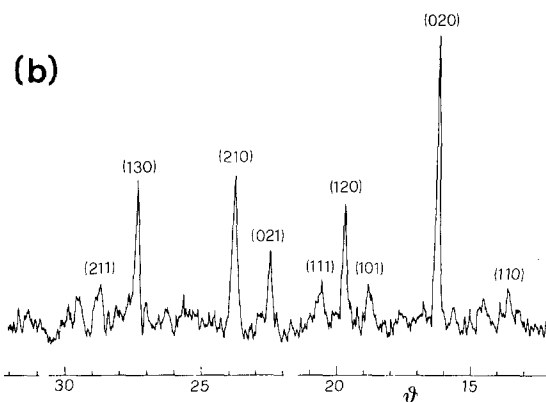
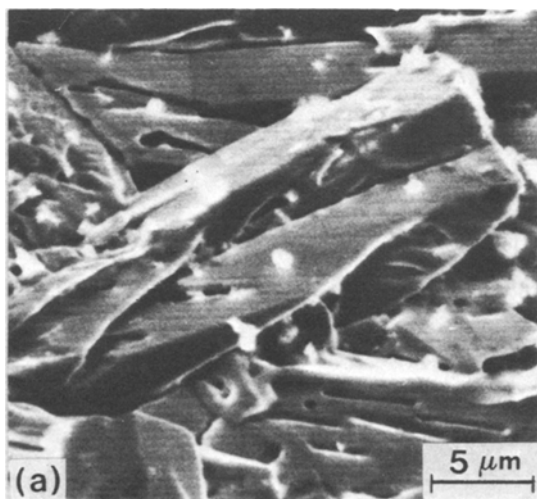


Figure 2 (a) SEM of the external surface of a boride layer grown on Armco iron in contact with crystalline boron powder for 15 h at  $1000^\circ\text{C}$ . (b) The corresponding X-ray diffraction pattern only shows resolved  $\text{FeB}$  diffraction peaks.

from the X-ray Mössbauer spectrum (Fig. 1c) a value of  $\sim 20\mu\text{m}$  was estimated for the total thickness of the boride layer. Hence it follows that the fracture surface ran into the inner  $\text{Fe}_2\text{B}$  layer, whose thickness is of  $\sim 15\mu\text{m}$ .

### 3.2. Morphology and mechanical consistency of borided layers

Fig. 2a, taken in the SEM, clearly shows that a boronizing of 15 h at  $1000^\circ\text{C}$  in crystalline boron powder has led to the formation on Armco iron of an outer, porous layer of reaction products, incorporating both small and large crystals growing together in a specific configuration. The presence of a layer of  $\text{FeB}$  is confirmed by the corresponding X-ray diffractogram in Fig. 2b. Obviously, X-ray diffraction was unable to confirm the formation of an external, very thin layer of the boron richer phase  $\text{FeB}_x$ . As already pointed out, a part of the boride layers break away under very low mechanical stresses, or spontaneously some time after the treatment. Fig. 3 shows a fractographic picture of this scale, whose thickness has been estimated at about  $10\mu\text{m}$ .

In any case, the fracture propagated parallel to the external surface, revealing an inner, more fine-grained and mechanically consistent layer (Fig. 4a). X-ray diffraction confirmed  $\text{Fe}_2\text{B}$  as the only compound constituting this internal layer (Fig. 4b), but, unlike already quoted results existing in the literature [10, 13], no intensification of the (002) diffraction peak was found. This leads to exclude a transition region between

randomly oriented crystals and textured crystals of the same phase as a source of nucleation and growth of the fracture of the boride layers examined in the present work.

Generally, internal stresses of compression develop in  $\text{Fe}_2\text{B}$  layers [33], where single crystals could undergo deformation and fracture as illustrated by Taga and Yoshida [34]. By comparing Fig. 2 with Fig. 4, however, one can survey the remarkable differences existing between morphologies of the outer, descaled part and the inner part of the coating. Moreover, the scaled material was easily reduced to a powder, while the remainder appeared to be more adherent to the base metal. In this case, therefore, one can realize a break-away in the  $\text{Fe}_2\text{B}$  layers, along fracture paths appearing to lie between  $\text{Fe}_2\text{B}$  regions of different mechanical consistency. Interfaces between different solid phases being well known as preferred regions for cracks to nucleate and propagate, it can be considered that porosity has allowed different phases to mutually accommodate at the  $\text{Fe}_2\text{B}$ – $\text{FeB}$  interface, while stress-relieving was ensured at the underlying  $\text{Fe}_2\text{B}$ – $\text{Fe}$  interface by the ductility of the base metal.

Optical metallography of cross-sections of the borided samples supports this view (Fig. 5), in that it shows a fracture surface running about parallel to the external surface and well within the boride coating, and shows moreover tooth-like penetrations of the base metal by reaction products.

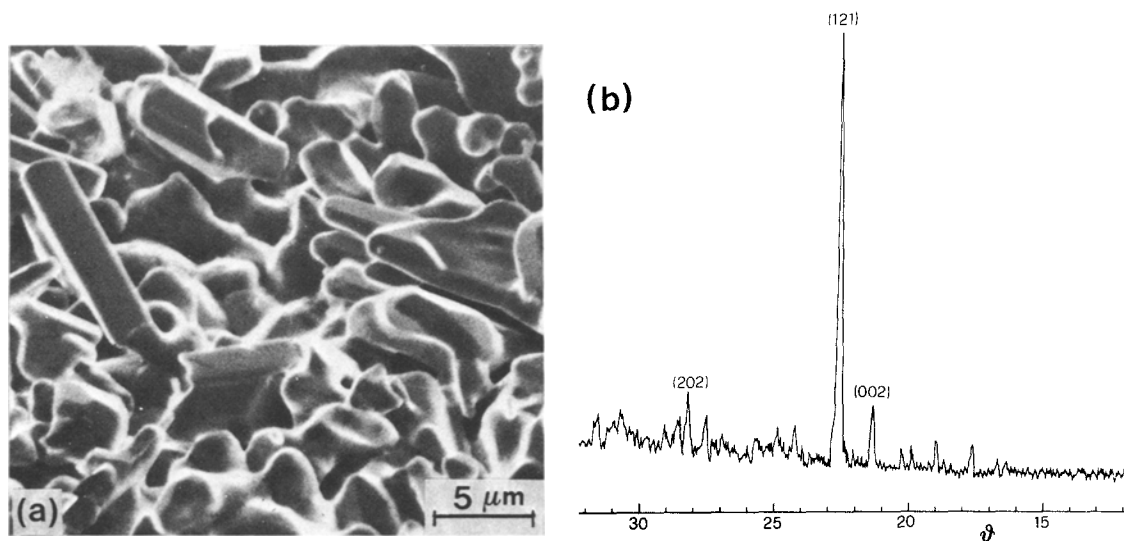


Figure 4 (a) SEM of the inner boride layer revealed after detaching of the outer layer shown in Fig. 3. (b) The corresponding X-ray diffraction pattern only shows resolved  $\text{Fe}_2\text{B}$  diffraction peaks.

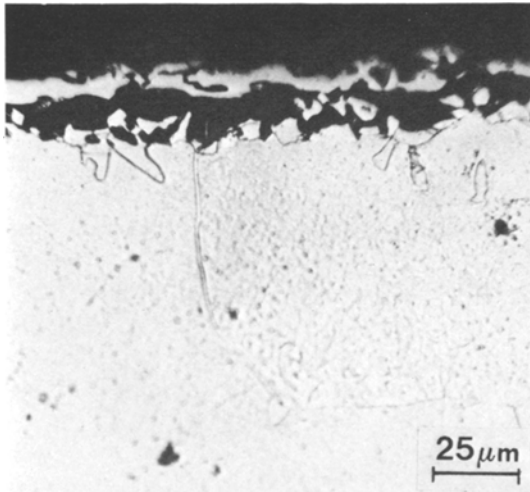


Figure 5 An optical micrograph of a cross-section of an Armco iron sample borided as reported in Fig. 2, showing the break-away of an outer part of the boride layer and the tooth-like penetrations of the base metal by the boride  $\text{Fe}_2\text{B}$ .

#### 4. Conclusions

As expected, boronizing of Armco iron samples in crystalline boron powder did not appear to be a surface treatment of practical importance, being unable to give rise to any reaction product in 24 h at  $850^\circ\text{C}$ , while in 15 h at  $1000^\circ\text{C}$  a surface coating has grown not thicker than  $20\ \mu\text{m}$  and too coarse-grained in microstructure. Mössbauer measurements, however, allowed this slow thermochemical process to be studied qualitatively and quantitatively, and some results of more general interest to be collected.

Three different iron–boron compounds have been identified in the boride coatings: from the base metal to the external surface, layers of  $\text{Fe}_2\text{B}$ ,  $\text{FeB}$  and  $\text{FeB}_x$  with  $x > 1$  followed one upon the other. It is worth noting that the studies published up to now on iron boriding generally ignore the presence of an outer, very thin layer of a third phase  $\text{FeB}_x$  above the  $\text{Fe}_2\text{B}$  and  $\text{FeB}$  layers which are always quoted.

Not only all the boride phases have been identified, but also the multi-layer structure of the reaction products was ascertained and the average thickness of each layer was measured in a fully non-destructive way, where metallography and X-ray diffraction analysis were unable to lead to equally complete results. After 15 h of powder boronizing at  $1000^\circ\text{C}$ , in particular, values of

$\sim 15\ \mu\text{m}$ ,  $\sim 5\ \mu\text{m}$  and  $\sim 30\ \text{nm}$  have been found, respectively, for the inner layer of  $\text{Fe}_2\text{B}$ , the intermediate layer of  $\text{FeB}$  and the outer layer of  $\text{FeB}_x$ .

The  $\text{Fe}_2\text{B}$  layers have shown a marked tendency to break along a path running about parallel to the external surface. The minimum strength of this path has been attributed to differences in mechanical consistency existing between adjacent regions of the same reaction product,  $\text{Fe}_2\text{B}$ , while in this case, owing to the lack of preferred orientations in  $\text{Fe}_2\text{B}$  layers, any contribution of texture anisotropy to descaling could be excluded.

#### Acknowledgements

The authors wish to thank Dr G. Sambogna, University of Bologna, for help and advice, and are particularly grateful to Professor F. Trifirò, University of Bologna, for encouragement to begin this work.

#### References

1. T. S. EYRE, *Wear* **34** (1975) 353.
2. K. H. HABIG, *Z. Werkstech.* **8** (1977) 267.
3. K. H. HABIG and H. KUNST, *Hart. -Tech. Mitt.* **30** (1975) 99.
4. R. H. BIDDULPH, *Thin Solid Films* **45** (1977) 341.
5. W. CHOMKA, W. DOWDA and L. NOWAK, *Hutnik (Katowice)* **42** (1975) 162.
6. M. A. KRISHTAL and E. M. GRINBERG, *Met. Sci. Heat Treat.* **16** (1974) 283.
7. T. KATAGIRI and N. TAKAMOTO, *Nippon Kinzoku Gakkai-Si* **32** (1968) 1245.
8. K. FUJII, T. KATAGIRI and Y. ITO, *J. Met. Finish. Soc. Japan* **28** (1977) 407.
9. L. S. LYAKHOVICH, B. M. KHUSID and Yu. V. TUROV, *Izvest. Akad. Nauk Beloruss. SSR (Fiz. -Tekhn.)* **1** (1975) 40.
10. L. S. LYAKHOVICH, F. V. DOLMANOV, V. V. SURKOV and Yu. V. TUROV, *Khim. -Termich. Obrabot. Met. Splavov*, Russian Collection, Minsk (1971) p. 74.
11. L. S. LYAKHOVICH, V. V. SURKOV, F. V. DOLMANOV and Yu. V. TUROV, *Met. Sci. Heat Treat.* **13** (1972) 608.
12. L. S. LYAKHOVICH, L. N. KOSACHEVSKY, A. Ya. KULIK, V. V. SURKOV and Yu. A. TUROV, *Zashch. Pokrytiya Metallakh*, Russian Collection, Kiev, Vol. 7 (1973) p. 80.
13. P. CASADESUS, C. FRANTZ and M. GANTOIS, *Mém. Sci. Rev. Mét.* **76** (1976) 9.
14. B. KASTNER and K. PRZYBYLOWICZ, *Hutnik (Katowice)* **44** (1977) 85.
15. M. CARBUCICCHIO, *Nucl. Instrum. Meth.* **144** (1977) 225.
16. A. M. GRISHIN and V. P. SENTYUREV, *Met. Sci. Heat Treat.* **17** (1975) 1049.
17. R. A. KRAKOWSKI and R. B. MILLER, *Nucl. Instrum. Meth.* **100** (1972) 93.



18. J. H. TERREL and J. J. SPIJKERMAN, *Appl. Phys. Letters* **13** (1968) 1.
19. J. M. THOMAS, M. J. TRICKER and P. A. WINTERBOTTOM, *J. Chem. Soc. Faraday II* **71** (1975) 1708.
20. V. E. COSSLETT and R. N. THOMAS, *Brit. J. Appl. Phys.* **15** (1964) 883.
21. A. BROWN, J. D. GARNISH and R. W. K. HONEYCOMBE, *Met. Sci.* **8** (1974) 317.
22. H. BUNZEL, E. KREBER and U. GONSER, *J. Phys. (Paris)* **35** (1974) C6.609.
23. J. VINCZE, M. CADEVILLE, R. JESSER and L. TAKACS, *ibid.* **35** (1974) C6.533.
24. T. SHIGEMATSU, *J. Phys. Soc. Japan* **39** (1975) 1233.
25. I. D. WEISMAN, L. J. SWARTZENDRUBER and L. H. BENNETT, *Phys. Rev.* **177** (1969) 465.
26. L. TAKACS, *Solid State Commun.* **21** (1977) 611.
27. T. SHINJO, E. JTOH, H. TAKAKI, Y. NAKAMURA and N. SHIKAZONO, *J. Phys. Soc. Japan* **19** (1964) 1252.
28. R. WÄPPLING, L. HÄGGSTRÖM and S. DEVANARAYANAN, *Phys. Scr.* **5** (1972) 97.
29. W. K. CHOO and R. KAPLOW, *Met. Trans. A8* (1977) 417.
30. V. V. DROBIT, O. N. TKACH and V. F. SHATINSKII, *Visn. L'viv. Politekh. Inst.* **91** (1975) 49.
31. K. I. PORTNOI, M. Kh. LEVINSKAYA and V. M. ROMASHOV, *Sov. Powder Met. Metal Ceram.* **8** (1969) 657.
32. B. CALLMER and T. LUNDSTRÖM, *J. Solid State Chem.* **17** (1976) 165.
33. M. RILE, *Met. Sci. Heat Treat.* **16** (1974) 836.
34. H. TAGA and H. YOSHIDA, *J. Mater. Sci.* **10** (1975) 1971.

Received 22 June and accepted 24 July 1979.